Sliding Contact Between a Cylindrical Punch and a Graded Half-Plane With an Arbitrary Gradient Direction

Chen Peijian
School of Mechanics and Civil Engineering,
State Key Laboratory for Geomechanics
and Deep Underground Engineering,
China University of Mining and Technology,
Xuzhou, Jiangsu 221116, China

Chen Shaohua[1]
LNM, Institute of Mechanics,
Chinese Academy of Sciences,
Beijing 100190, China
e-mail: shchen@LNM.imech.ac.cn;
chenshaohua72@hotmail.com

Peng Juan
School of Sciences,
China University of Mining and Technology,
Xuzhou, Jiangsu 221116, China

Contact behavior of a rigid cylindrical punch sliding on an elastically graded half-plane with shear modulus gradient variation in an arbitrary direction is investigated. The governing partial differential equations and the boundary conditions are achieved with the help of Fourier integral transformation. As a result, the present problem is reduced to a singular integral equation of the second kind, which can be solved numerically. Furthermore, the presently general model can be well degraded to special cases of a lateral gradient half-plane and a homogeneous one. Normal stress in the contact region is predicted with different material parameters, which is usually used to estimate the possibility of surface crack initiation. The moment that is needed to ensure stable sliding of the cylindrical punch on the contact surface is further predicted. The result in the present paper should be helpful for the design of novel graded materials with surfaces of strong abrasion resistance. [DOI: 10.1115/1.4029781]

Keywords: sliding contact mechanics, graded material, arbitrarily oriented gradient, abrasion

1 Introduction

Gradient property in materials is widely found in stratigraphic and biological structures, for examples, soil, bamboos, plant stems, teeth, and bones, which gives them special mechanical characteristics, in contrast to the corresponding homogeneous ones [1,2]. Inspired by nature, human beings increasingly aim to fabricate functionally graded materials (FGMs) with some unique features, such as thermo-shock resistance, antiwear performance, oxidation resistance, hardness, even surface, or interface adhesive strength, which would be appreciated in the field of advanced manufacturing industry, aerospace, biomimetic fabrication, automotive engineering, and so on. Surface contact of such gradient materials is unavoidably involved, no matter with gas, liquid, or solid. How to assess the surface properties, especially the surface abrasion resistance, is one of the important problems in the design of novel graded materials. As an effective technique, indentation and scratch hardness tests are usually adopted to measure surface properties of homogeneous materials and now extended to predict surface characteristics of graded materials [3–5].

Generally, gradient of graded materials is often described by the Young's modulus or the shear one varying in depth according to a power or exponential law with Poisson's ratio remaining a constant. On the premise of this assumption, many researches have been carried out. With regard to an axisymmetric contact problem of a graded half-space subjected to a concentrated force, or a flat, spherical or conical punch, Giannakopoulus and Suresh [6,7] found that stress distributions in the frictionless contact region could be significantly influenced by gradient features. Guler and Erdogan [8–10] studied the frictional contact problem of an FGM-coated substrate punched by a rigid indenter and the contact one of two deformable solids with graded coatings. Receding contact between a functionally graded coating and a homogeneous substrate was investigated by El-Borgi and his coworkers [11,12]. Choi and Paulino [13,14] analyzed a thermo-elastic contact problem of a coating/substrate system with graded properties and the corresponding one coupled with a crack, respectively. A linearly multilayered model was proposed by Wang and his colleagues to analyze contact problems of graded materials [15,16]. In order to find difference between an infinite graded model and a finite one, contact properties of FGM with a finite size were studied by the present authors [17–19].

All the above belong to Hertz contact mechanics without considering the interface adhesion. Several typical models should be mentioned for graded materials while the interface adhesion is included. A plane strain adhesive contact model of a rigid cylinder on an elastically graded substrate was studied by Giannakopoulos and Pallot [20]. Further discussion on the plane strain adhesive model was given by Chen et al. [21]. As for a rigid sphere in adhesive contact with a graded half-space, a very simple closed-form analytical solution was achieved by Chen et al. [22], which could be well reduced to the classical Johnson–Kendall–Roberts (JKR) solution as well as that for Gibson soil materials. Considering a similar JKR-Derjaguin–Muller–Toporov (DMT) transition, axis-symmetrically adhesive contact models for graded half-spaces were further analyzed by Guo et al. [23] and Jin et al. [24,25].

Both the above Hertz contact models and the adhesive ones are related to graded materials with gradient varying in depth, i.e., perpendicular to the contact surface. How is it about graded materials with gradient varying in other directions? Fortunately, a few studies were found, in which the gradient variation of graded materials is horizontal, i.e., parallel to the contact surface [26,27], which is still a special one in contrast to cases with gradient varying in an arbitrary direction. Such cases cannot be avoided in real applications, for example, nonuniform foundation settlement, asymmetric indentation, even for teeth in the process of chewing.

In the present paper, a more generalized Hertz contact model is established for graded materials with gradient variation in an arbitrary direction, which can be well degraded into the existing special cases, i.e., those of a homogeneous half-plane and a laterally graded one. In the present model, interfacial friction between the cylindrical punch and the graded half-plane and the moment in order to keep the punch vertically to the contact interface are considered besides the normal loading. Fourier integral transform method is adopted to obtain the normal traction and the in-plane

[1]Corresponding author.

Manuscript received January 21, 2015; final manuscript received February 9, 2015; published online February 26, 2015. Editor: Yonggang Huang.

surface stress, which can be used to access the surface abrasion resistance. Effects of different parameters and different varying trends of the shear modulus gradient on distributions of the normal traction and the in-plane stress are investigated and discussed. The results in the present paper should be useful in the analysis of real applications and for the design of novel graded materials.

2 Contact Model and Theoretical Analysis

Hertz sliding contact between a rigid cylindrical punch of radius R and a graded half-plane with gradient varying in an arbitrary direction is studied in the present paper. A plane contact model is established as shown in Fig. 1, in which the contact width is from $x = -a$ to $x = b$ at the surface $x = 0$, asymmetric with respect to the line $x = 0$. Coulomb friction is adopted at the contact interface. The shear modulus μ of the graded half-plane is assumed to vary exponentially in an arbitrary direction denoted by θ, an angle deviating from the direction of depth, with an assumption of Poisson's ratio ν remaining constant. Then, in the (x', y') coordinate system, we have

$$\mu(y') = \mu_0 e^{\delta y'} \tag{1}$$

In the (x, y) coordinate system, it is written as

$$\mu(x, y) = \mu_0 e^{\beta x + \gamma y} \tag{2}$$

where

$$\beta = -\delta \sin\theta = -\frac{\delta \tan\theta}{\sqrt{1 + \tan^2\theta}} \tag{3}$$

$$\gamma = \delta \cos\theta = \frac{\delta}{\sqrt{1 + \tan^2\theta}} \tag{4}$$

The subscript "0" denotes the surface layer, and μ_0 and δ are two material constants. For the special case of a homogeneous half-plane, we have $\delta = 0$, i.e., $\beta = 0$ and $\gamma = 0$.

Hooke's law is still valid for the elastically graded half-plane, i.e.,

$$\sigma_{xx} = \frac{\mu}{\kappa - 1}\left[(1 + \kappa)\frac{\partial u}{\partial x} + (3 - \kappa)\frac{\partial v}{\partial y}\right] \tag{5a}$$

$$\sigma_{yy} = \frac{\mu}{\kappa - 1}\left[(1 + \kappa)\frac{\partial v}{\partial y} + (3 - \kappa)\frac{\partial u}{\partial x}\right] \tag{5b}$$

$$\sigma_{xy} = \mu\left[\frac{\partial u}{\partial y} + \frac{\partial v}{\partial x}\right] \tag{5c}$$

where σ_{ij} (i or $j = x$ or y) denotes stress components. $u(x, y)$ and $v(x, y)$ are displacement components in x and y directions. $\kappa = 3 - 4\nu$ for a plane strain model and $\kappa = (3 - \nu)/(1 + \nu)$ for a plane stress one.

Substituting Eqs. (5a)–(5c) into equilibrium equations yields

$$(\kappa + 1)\frac{\partial^2 u}{\partial x^2} + (\kappa - 1)\frac{\partial^2 u}{\partial y^2} + 2\frac{\partial^2 v}{\partial x \partial y} + \beta(\kappa + 1)\frac{\partial u}{\partial x} + \gamma(\kappa - 1)\frac{\partial u}{\partial y} + \gamma(\kappa - 1)\frac{\partial v}{\partial x} + \beta(3 - \kappa)\frac{\partial v}{\partial y} = 0 \tag{6a}$$

$$(\kappa - 1)\frac{\partial^2 v}{\partial x^2} + (\kappa + 1)\frac{\partial^2 v}{\partial y^2} + 2\frac{\partial^2 u}{\partial x \partial y} + \gamma(3 - \kappa)\frac{\partial u}{\partial x} + \beta(\kappa - 1)\frac{\partial u}{\partial y} + \beta(\kappa - 1)\frac{\partial v}{\partial x} + \gamma(\kappa + 1)\frac{\partial v}{\partial y} = 0 \tag{6b}$$

The general solution of Eqs. (6a) and (6b) can be obtained with Fourier integral transformation technique

$$u(x, y) = \frac{1}{2\pi}\int_{-\infty}^{+\infty}\sum_{j=1}^{4} m_j B_j(\alpha) e^{n_j y - i\alpha x} d\alpha \tag{7a}$$

$$v(x, y) = \frac{1}{2\pi}\int_{-\infty}^{+\infty}\sum_{j=1}^{4} B_j(\alpha) e^{n_j y - i\alpha x} d\alpha \tag{7b}$$

where $n_j(\alpha)$ and $m_j(\alpha)$ ($j = 1, ..., 4$) are given in Appendix A, $B_j(\alpha)$ ($j = 1, ..., 4$) are unknown parameters to be determined by boundary conditions.

3 Boundary Conditions

The vertical displacement is known in advance within the contact area, which can be found from the profile function of cylindrical punches

$$v(x, 0) = h - \frac{(c - x)^2}{2R}, \quad -a \le x \le b \tag{8}$$

where h is a vertical translation of the rigid cylindrical punch, and c denotes the centerline position of the punch, as shown in Fig. 1.

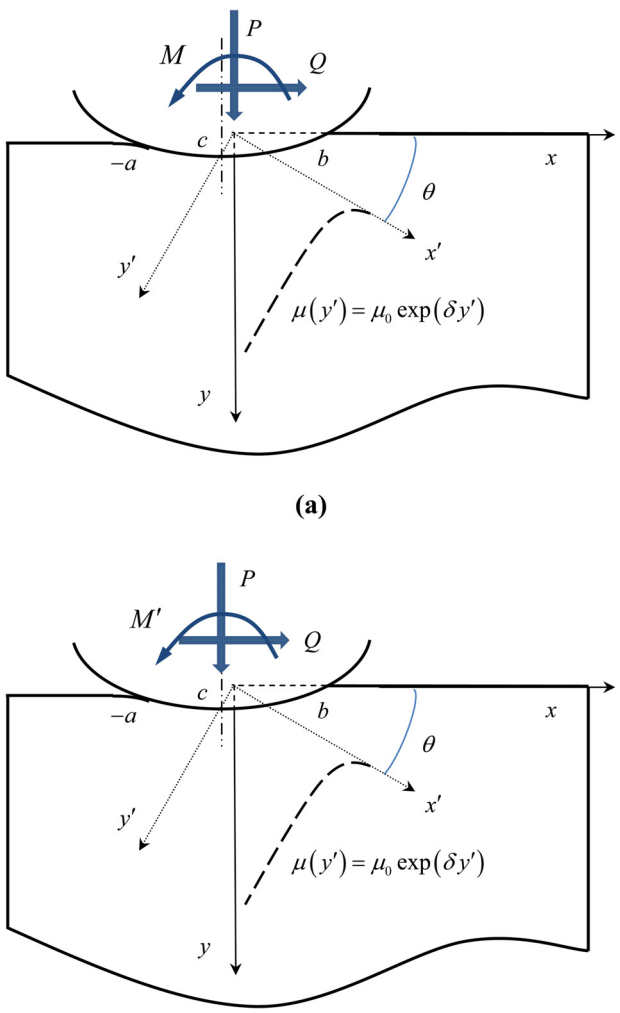

Fig. 1 The Hertzian contact model of a rigid cylindrical punch sliding on a graded half-plane with an arbitrarily gradient orientation. (*a*) External loads induce an asymmetric contact width with respect to the coordinate system; (*b*) shifting the normal load to the centerliner of contact punch $x = c$ induces a variation of the moment needed by the rigid punch for stable sliding.

The tangential and normal tractions beneath the punch abide by the Coulomb friction law

$$\sigma_{xy}(x,0) = \mu_f \sigma_{yy}(x,0), \quad -a \le x \le b \tag{9}$$

The resultant force P and moment applied to the punch as shown in Fig. 1(*a*) will be

$$\int_{-a}^{b} \sigma_{yy}(x,0)\mathrm{d}x = -P, \quad -a \le x \le b \tag{10}$$

$$\int_{-a}^{b} \sigma_{yy}(x,0)x\mathrm{d}x = -M, \quad -a \le x \le b \tag{11a}$$

Moving the loading to the centerline of the punch yields an effective moment

$$\int_{-a}^{b} \sigma_{yy}(x,0)(x-c)\mathrm{d}x = -M', \quad -a \le x \le b \tag{11b}$$

where we have $M' = M - Pc$, as shown in Fig. 1(*b*).

Although there will be translation or rotation in general circumstances, considering the case that the punch moves parallel to the y-axis without rotation is still of great significance to explain many physical phenomena [28].

Outside the contact region, we have

$$\sigma_{yy}(x,0) = \sigma_{xy}(x,0) = 0, x < -a, \quad x > b \tag{12}$$

and the normal and tangential displacements should vanish for $y \to +\infty$

$$u(x,+\infty) = v(x,+\infty) = 0 \tag{13}$$

4 Solution of the Surface Contact Tractions

Similar to Chen and Chen [29], Fourier transform method yields the derivative of displacement fields $u(x,y)$ and $v(x,y)$.

$$\frac{\partial u(x,0)}{\partial x} = \frac{\kappa-1}{4}\frac{\sigma_{yy}(x,0)}{\mu} - \frac{\kappa+1}{4\pi}\int_{-a}^{b}\frac{1}{r-x}\frac{\sigma_{xy}(r,0)}{\mu}\mathrm{d}r + \frac{1}{\pi}\int_{-a}^{b}\left[K_{11}(x,r)\frac{\sigma_{xy}(r,0)}{\mu} + K_{12}(x,r)\frac{\sigma_{yy}(r,0)}{\mu}\right]\mathrm{d}r \tag{14}$$

$$\frac{\partial v(x,0)}{\partial x} = -\frac{\kappa-1}{4}\frac{\sigma_{xy}(x,0)}{\mu} - \frac{\kappa+1}{4\pi}\int_{-a}^{b}\frac{1}{r-x}\frac{\sigma_{yy}(r,0)}{\mu}\mathrm{d}r + \frac{1}{\pi}\int_{-a}^{b}\left[K_{21}(x,r)\frac{\sigma_{xy}(r,0)}{\mu} + K_{22}(x,r)\frac{\sigma_{yy}(r,0)}{\mu}\right]\mathrm{d}r \tag{15}$$

where the kenerls $K_{ij}(x,r)$ are bounded functions given in Appendix B.

The surface traction inside the contact area can be rewritten as

$$\sigma_{yy}(x,0) = -p(x), \quad -a \le x \le b \tag{16}$$

$$\sigma_{xy}(x,0) = -\mu_f p(x), \quad -a \le x \le b \tag{17}$$

where $p(x)$ denotes the normal surface traction in the contact region.

Substituting Eqs. (16) and (17) into Eq. (15) leads to

$$\frac{\kappa-1}{4}\frac{\mu_f p(x)}{\mu} + \frac{1+\kappa}{4\pi}\int_{-a}^{b}\frac{1}{r-x}\frac{p(r)}{\mu}\mathrm{d}r - \frac{1}{\pi}\int_{-a}^{b}Q_1(x,r)\frac{p(r)}{\mu}\mathrm{d}r = \frac{\partial v(x,0)}{\partial x} \tag{18}$$

where $Q_1(x,r) = \mu_f K_{21}(x,r) + K_{22}(x,r)$.

Introducing nondimensional quantities

$$x = \frac{a+b}{2}s + \frac{b-a}{2}, \quad r = \frac{a+b}{2}t + \frac{b-a}{2}, \quad -a \le (x,r) \le b, \quad -1 \le (s,t) \le 1 \tag{19a}$$

$$P_1(x) = \frac{p(x)}{\exp(\beta x)} = -\frac{\sigma_{yy}(x,0)}{\exp(\beta x)} = \tilde{P}_1(s) \tag{19b}$$

Equations (18) and (10) can be rewritten as

$$\frac{\kappa-1}{1+\kappa}\mu_f\bar{P}_1(s) + \frac{1}{\pi}\int_{-1}^{1}\frac{\bar{P}_1(t)}{t-s}\mathrm{d}t - \frac{2(a+b)}{\pi(\kappa+1)}\int_{-1}^{1}Q_1(s,t)\bar{P}_1(t)\mathrm{d}t = \frac{4}{(1+\kappa)R}f(s) \tag{20}$$

$$\int_{-1}^{1}\bar{P}_1(t)\exp\left[\beta\cdot\left(\frac{a+b}{2}t + \frac{b-a}{2}\right)\right]\mathrm{d}t = g \tag{21}$$

where $\bar{P}_1(x) = \tilde{P}_1(s)/\mu_0$, $f(s) = c - a + b/2s - b - a/2$, and $g = 2P/(a+b)\mu_0$.

One can see that the Cauchy-type singular kernel exists in the integral equation. Then, the solution to Eqs. (20) and (21) can be given in terms of Jacobi Polynomials

$$\bar{P}_1(s) = w(s)\sum_{j=0}^{\infty}A_j P_j^{(\beta_1,\beta_2)}(s), \quad |s| \le 1 \tag{22}$$

in which $w(s) = (1-s)^{\beta_1}(1+s)^{\beta_2}$ and parameters A_j are unknown. $P_j^{(\beta_1,\beta_2)}(\cdot)$ are Jacobi Polynomials corresponding to the weight function $w(s)$. The superscripts β_1 and β_2 are determined from the physics of the contact problem

$$\beta_1 = \frac{1}{\pi}\mathrm{arccot}\left(-\mu_f\frac{\kappa-1}{\kappa+1}\right), \quad \beta_2 = \frac{1}{\pi}\mathrm{arccot}\left(\mu_f\frac{\kappa-1}{\kappa+1}\right) \tag{23}$$

where it is easily found that β_1 and β_2 depend only on the friction coefficient and Poisson's ratio.

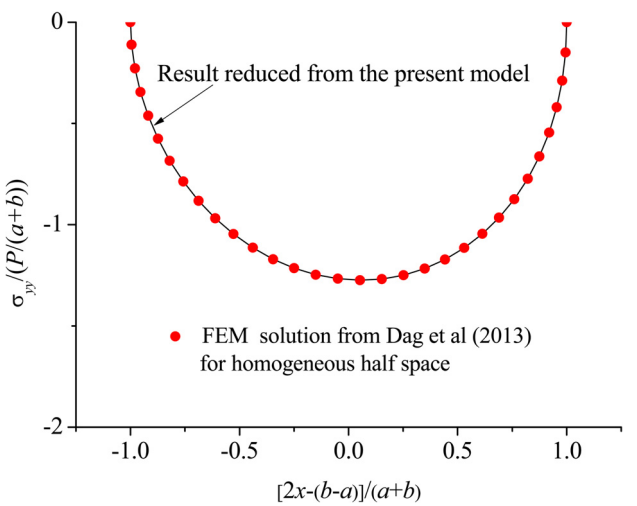

Fig. 2 Distribution of the normal traction $\sigma_{yy}(x,0)/(P/(a+b))$ in the contact model of a homogeneous half-plane with $\mu_f = 0$, where FEM results achieved by Dag et al. are given for comparison

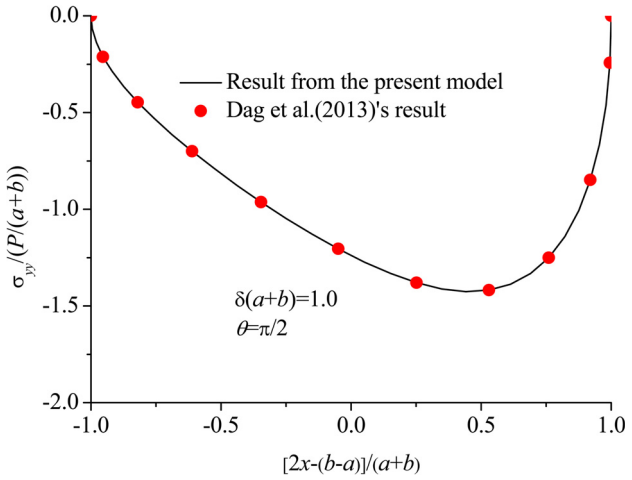

Fig. 3 Distribution of the normal traction $\sigma_{yy}(x,0)/(P/(a+b))$ in the contact model of a laterally graded half-plane with $\delta(a+b)=1.0$ and $\mu_f=0$, where FEM results achieved by Dag et al. are given for comparison

Considering the following property of Jacobi Polynomials:

$$\mu_f\frac{\kappa-1}{1+\kappa}w(s)P_j^{(\beta_1,\beta_2)}(s)+\frac{1}{\pi}\int_{-1}^{1}\frac{1}{s-t}w(t)P_j^{(\beta_1,\beta_2)}(t)\mathrm{d}t = -\frac{2}{\sin(\pi\beta_1)}P_{j+1}^{(-\beta_1,-\beta_2)}(s),\quad |s|\le 1 \tag{24}$$

and substituting Eq. (22) into Eqs. (20) and (21) yields

$$\sum_{j=0}^{\infty}\left[\frac{-2}{\sin(\pi\beta_1)}P_{j+1}^{(-\beta_1,-\beta_2)}(s)+Q_j^*(s)\right]A_j=\frac{4}{(1+\kappa)R}f(s) \tag{25}$$

$$\int_{-1}^{1}\sum_{j=0}^{\infty}w(t)P_j^{(-\beta_1,-\beta_2)}(t)\exp\left\{\frac{\beta}{2}[(a+b)t+(b-a)]\right\}A_j\mathrm{d}t=g \tag{26}$$

where

$$Q_j^*(s)=\frac{2(a+b)}{\pi(\kappa+1)}\int_{-1}^{1}Q_1(s,t)w(t)P_j^{(\beta_1,\beta_2)}(t)\mathrm{d}t \tag{27}$$

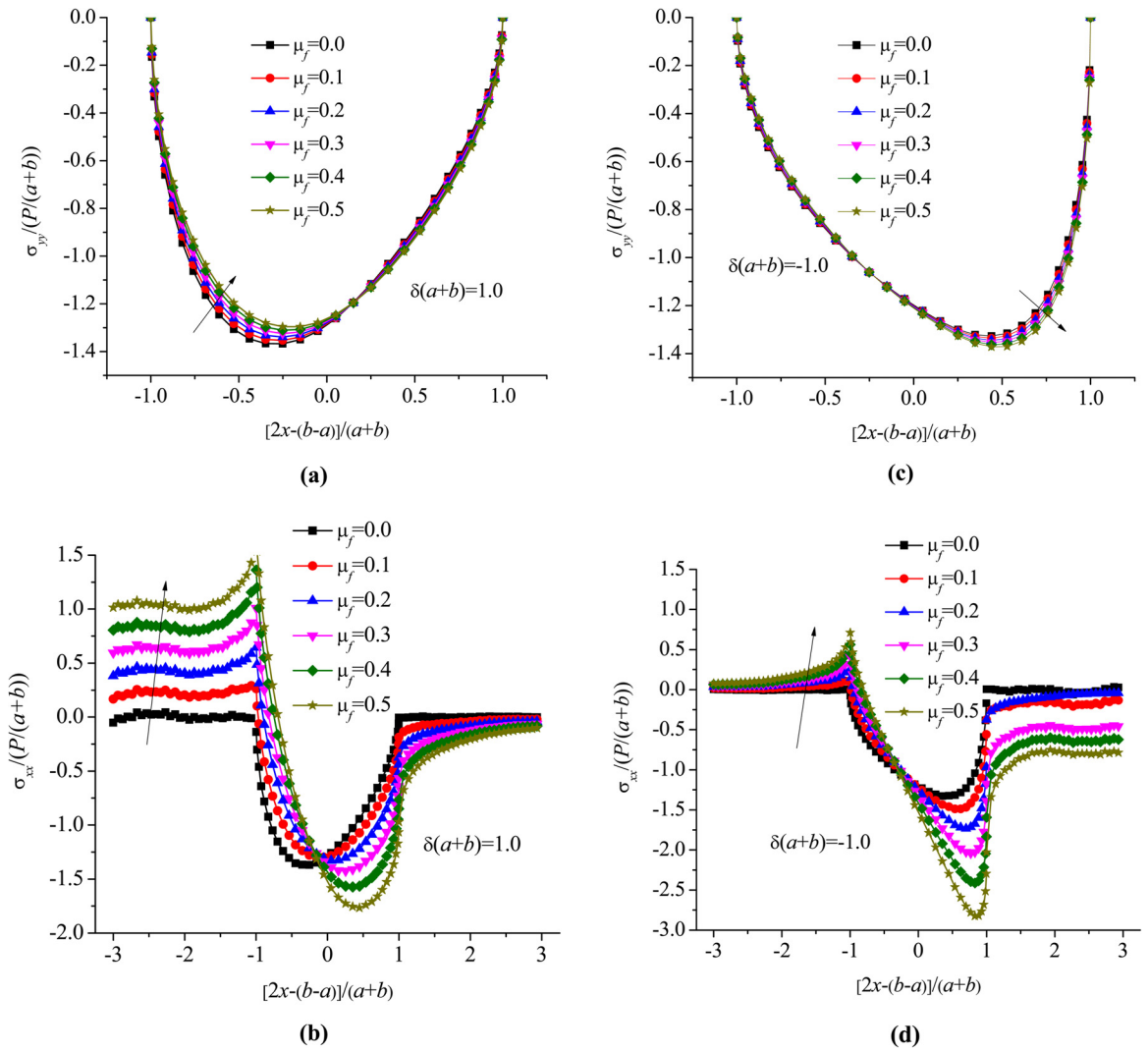

Fig. 4 Distribution of the normal traction $\sigma_{yy}(x,0)/(P/(a+b))$ and in-plane stress $\sigma_{xx}(x,0)/(P/(a+b))$ in the contact model of a graded half-plane with a gradient variation angle $\theta=0.3\pi$ and different surface friction coefficient μ_f. (*a*) and (*b*) For $\delta(a+b)=1.0$; (*c*) and (*d*) for $\delta(a+b)=-1.0$.

Taking into consideration the following orthogonality property of Jacobi Polynomials:

$$\int_{-1}^{1} w(t)P_j^{(\beta_1,\beta_2)}(t)P_k^{(\beta_1,\beta_2)}(t)\mathrm{d}t = \theta_j^{(\beta_1,\beta_2)}\delta_{jk}, \quad j,k = 0,1,2,... \tag{28}$$

where

$$\theta_j^{(\beta_1,\beta_2)} = \begin{cases} \displaystyle\int_{-1}^{1} w(t)\mathrm{d}t = \frac{2^{\beta_1+\beta_2+1}\Gamma(\beta_1+1)\Gamma(\beta_2+1)}{\Gamma(\beta_1+\beta_2+2)}, & j=0, \\ \displaystyle\frac{2^{\beta_1+\beta_2+1}\Gamma(j+\beta_1+1)\Gamma(j+\beta_2+1)}{(2j+\beta_1+\beta_2+1)j!\,\Gamma(j+\beta_1+\beta_2+1)}, & j\geq 1 \end{cases}$$

δ_{jk} is the Kronecker delta function, truncating series in Eq. (22) at $j = N-1$ and selecting collocation points s_m $(m = 1,2,...,N)$ as roots of the following Jacobi Polynomials:

$$P_N^{(-\beta_1,-\beta_2)}(s_m) = 0 \tag{29}$$

Equation (25) can be rewritten as

$$-\frac{2\theta_j^{(-\beta_1,-\beta_2)}}{\sin(\pi\beta_1)}A_{j-1} + \sum_{k=0}^{N-1} d_{jk}A_k = f_j \tag{30}$$

where

$$f_j = \frac{4}{(1+\kappa)R}\int_{-1}^{1} P_j^{(-\beta_1,-\beta_2)}(s)\left(c - \frac{a+b}{2}s - \frac{b-a}{2}\right)(1-s)^{-\beta_1}(1+s)^{-\beta_2}\mathrm{d}s \tag{31a}$$

$$d_{jk} = \int_{-1}^{1} Q_j^*(s)P_k^{(-\beta_1,-\beta_2)}(s)(1-s)^{-\beta_1}(1+s)^{-\beta_2}\mathrm{d}s \tag{31b}$$

It is readily found that Eqs. (26) and (30) consist of $N+1$ linear algebraic equations for $N+1$ unknown constants A_j $(j = 0, 1, ..., N-1)$ and c (or P). Based on the solution of Eqs. (26) and (30), $p(x)$ in Eq. (19b) can be approximately given as

$$p(x) = \mu_0\exp(\beta x)\left(1 - \frac{2x-(b-a)}{a+b}\right)^{\beta_1} \times \left(1 + \frac{2x-(b-a)}{a+b}\right)^{\beta_2}\sum_{j=0}^{N-1} A_j P_j^{(\beta_1,\beta_2)}\left(\frac{2x-(b-a)}{a+b}\right) \tag{32}$$

Then, the in-plane stress $\sigma_{xx}(x,0)$ near the surface can be obtained from Eq. (5a) and Eqs. (14) and (15) as

$$\sigma_{xx}(x,0) = -p(x) + \frac{2\mu_f}{\pi}\int_{-a}^{b}\frac{1}{r-x}p(r)\mathrm{d}r - \frac{8}{\pi(\kappa+1)}\int_{-a}^{b} Q_2(x,r)p(r)\mathrm{d}r \tag{33}$$

where $Q_2(x,r) = K_{11}(x,r) + \mu_f K_{12}(x,r)$.

Furthermore, the moment can then be achieved easily from Eq. (11a) or (11b).

5 Results and Discussion

In all calculations of the present paper, we take $\nu = 0.3$ due to a negligible effect of Poisson's ratio on the contact behavior [2,6,7]. The normal traction and the in-plane contact stress in the contact region as well as the moment needed to keep punch moving vertically are focused on.

From above, one can see that three parameters are related to the heterogeneity of the graded half-space, i.e., the contact widths $-a$ and b, and the gradient index δ. Inspired by Dag et al. [26], it is reasonable for us to combine three separated parameters into two nondimensional ones $\delta(a+b)$ and $\delta(b-a)$. Furthermore, $\delta(b-a)$ is fixed as zero according to Fig. 1(b) and $\delta(a+b)$ is only taken as a variable for convenience.

Special Case I. If we set $\delta = 0$ in our model, it will be reduced to a special case that is a rigid punch in contact with a homogeneously elastic half-plane. Distribution of the corresponding nondimensionally normal traction $\sigma_{yy}/(P/(a+b))$ is shown in Fig. 2, which is bounded at both contact edges and consistent well with existing finite element method (FEM) results [27]. Closed-form solution for such a special case can be further found in the Appendix.

Special Case II. If we take $\theta = \pi/2$, our model will then be degraded into another special case that is a rigid punch contacting a graded half-plane with gradient variation in the horizontal direction [27]. Comparison of the result predicted by the present model and that in Dag et al. [27] exhibits good agreement as shown in Fig. 3.

General Cases. Distributions of the normal traction and in-plane surface stress are shown in Figs. 4(a)–4(d) for cases with different friction coefficients μ_f but with a fixed gradient variation angle $\theta = 0.3\pi$. Furthermore, the value of parameter $\delta(a+b)$ in Figs. 4(a) and 4(b) is different from that in Figs. 4(c) and 4(d),

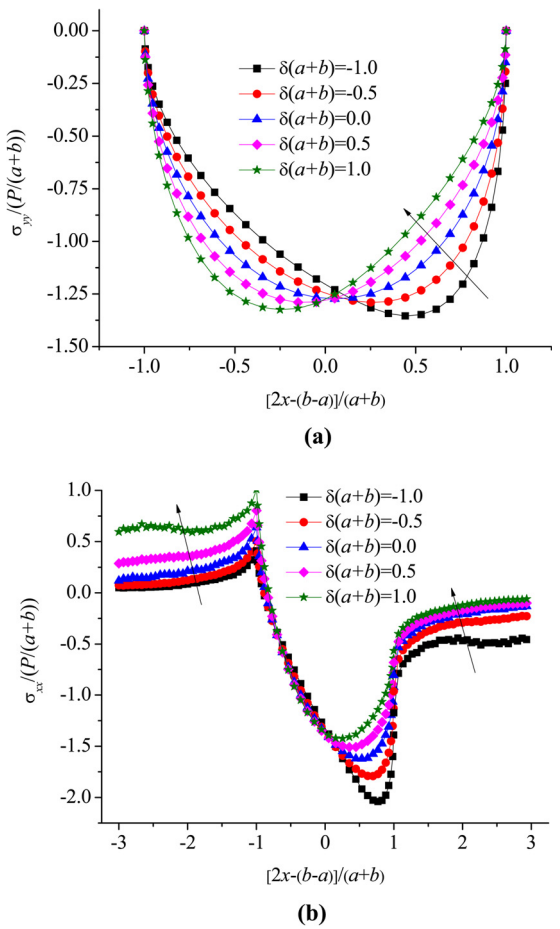

Fig. 5 Distribution of the interface stresses inside the contact region in the contact model of a graded half-plane with $\theta = 0.3\pi$, $\mu_f = 0.3$, and different values of $\delta(a+b)$. (a) For the normal traction $\sigma_{yy}(x,0)/(P/(a+b))$; (b) for the in-plane stress $\sigma_{xx}(x,0)/(P/(a+b))$.

where a positive value of $\delta(a+b)$ denotes Young's modulus of the graded half-plane increasing from the surface to within in the direction of gradient variation angle θ, while a negative value of $\delta(a+b)$ is a reversal. Comparing the case with a positive $\delta(a+b)$ and that with a negative one, not only the normal traction but also the in-plane stress distributes asymmetrically with respect to the axis $x=0$. In cases with a positive $\delta(a+b)$ as shown in Figs. 4(*a*) and 4(*b*), the normally compressive traction decreases with an increasing friction coefficient, while the in-plane stress at the trailing edge is a tensile one and increases with the friction coefficient increasing. By comparison, in cases with a negative $\delta(a+b)$ as shown in Figs. 4(*c*) and 4(*d*), both the normally compressive traction and the in-plane tensile stress at the trailing edge increase with an increasing friction coefficient, but the magnitude of in-plane tensile stress is much smaller than that in cases with a positive $\delta(a+b)$. It is interesting to find that, in both cases, the in-plane stress is compressive at the leading edge and increases with the friction coefficient increasing as shown in Figs. 4(*b*) and 4(*d*). Generally, in a sliding contact system, cracks always unavoidably emerge on the contact surface, which are actually induced by the in-plane tensile stress. Therefore, it is reasonable to infer that a small friction coefficient should be favorable to relieve surface contact damage, consistent with the common sense.

Distributions of the normal traction and the in-plane stress influenced by the value of parameters $\delta(a+b)$ are shown in Figs. 5(*a*) and 5(*b*) with a determined friction coefficient $\mu_f=0.3$ and gradient variation angle $\theta=0.3\pi$, respectively. It is found that the value of $\delta(a+b)$ has significant influence on the normal traction. The skewing direction is totally opposite for cases of $\delta(a+b)>0$ and those of $\delta(a+b)<0$ as shown in Fig. 5(*a*). A graded half-space with stiffness decreasing in the gradient variation direction, i.e., $\delta(a+b)<0$, will have less possibility for crack initiation as shown in Fig. 5(*b*), which agrees qualitatively with the conclusion given in Refs. [8] and [13]. Interestingly, such a strategy has already been adopted by many natural biomaterials, for instance, teeth and bones.

Figure 6 gives the effect of gradient variation angles θ on the distribution of normal traction and in-plane stress with a fixed friction coefficient $\mu_f=0.3$. Figures 6(*a*) and 6(*b*) correspond to a graded half-plane with stiffness decreasing in the gradient variation direction, i.e., $\delta(a+b)<0$, while Figs. 6(*c*) and 6(*d*) correspond to the one with stiffness increasing in the gradient variation direction, i.e., $\delta(a+b)>0$. No solution can be found when $\theta=0$ for a graded half-plane with stiffness decreasing in the gradient variation direction, which is consistent with the finding in Ref. [30]. With other gradient variation angles θ, it is found that the skewing of distribution of the normal traction is enhanced by an increasing θ in cases with $\delta(a+b)<0$ as shown in Fig. 6(*a*), while it is reduced for $\delta(a+b)>0$ as shown in Fig. 6(*c*). The gradient variation angle shows a more obvious effect on the in-plane compressive stress near the leading edge than the in-plane tensile stress near the trailing edge in cases with $\delta(a+b)<0$ and the in-plane compressive stress increases with an increasing gradient variation angle as shown in Fig. 6(*b*), while the in-plane compressive stress decreases with the gradient variation angle increasing as shown in Fig. 6(*d*). An interesting phenomenon is that the maximal tensile stress near the trailing edge does not

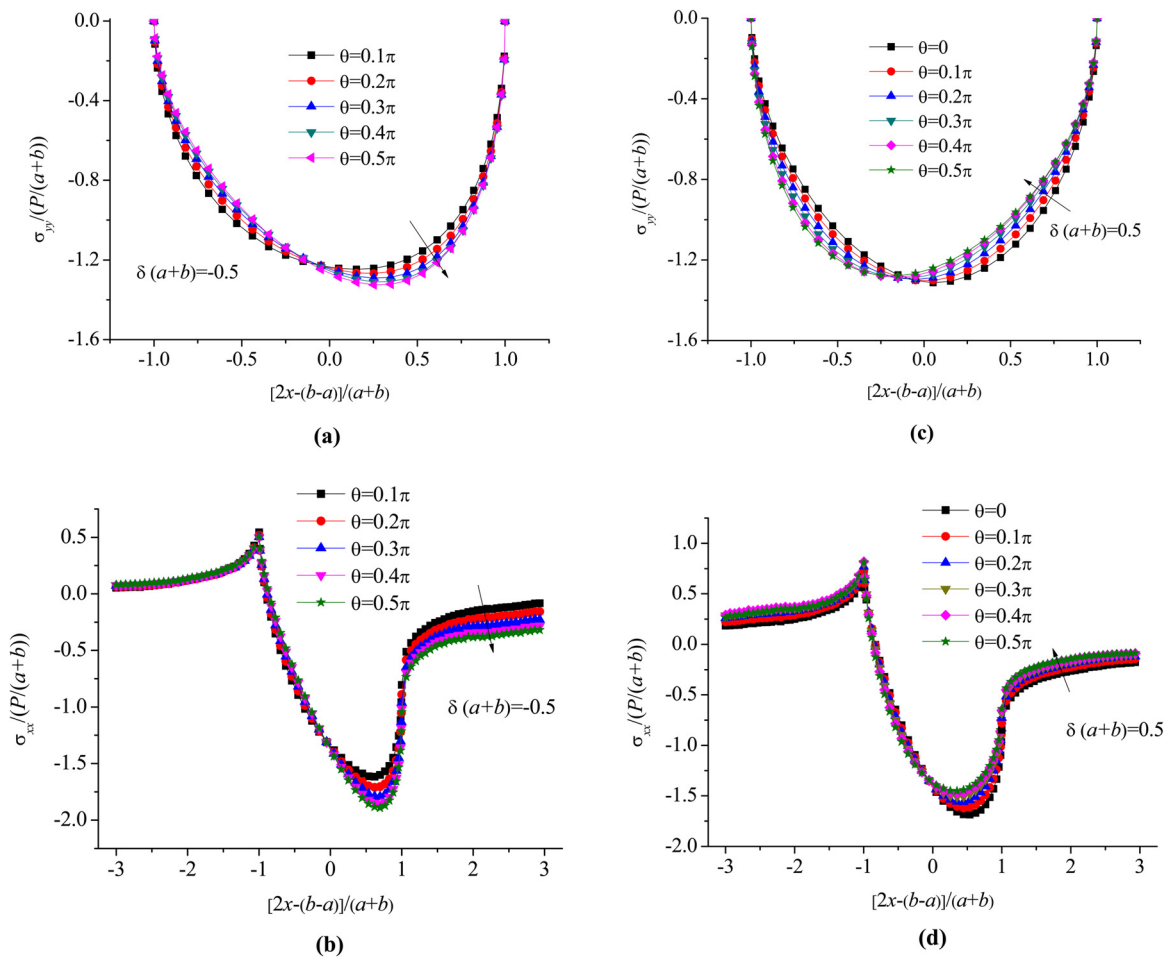

Fig. 6 Distribution of the normal traction $\sigma_{yy}(x,0)/(P/(a+b))$ and in-plane stress $\sigma_{xx}(x,0)/(P/(a+b))$ in the contact model of a graded half-plane with $\mu_f=0.3$ and different gradient variation angles θ. (*a*) and (*b*) For $\delta(a+b)=-0.5$; (*c*) and (*d*) for $\delta(a+b)=0.5$.

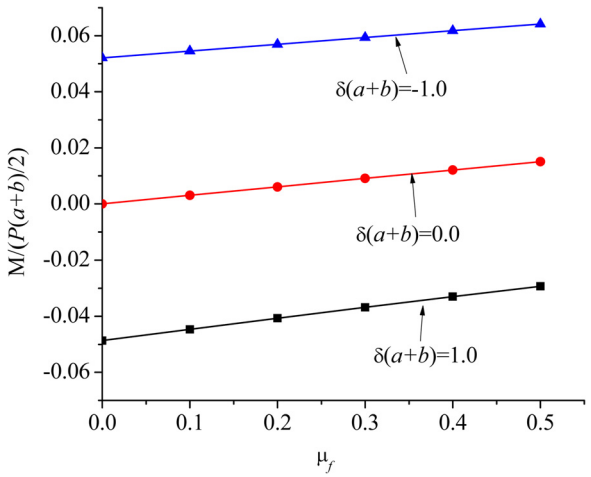

Fig. 7 Variations of the nondimensional moment $M/[P(a+b)/2]$ versus the friction coefficient μ_f for some selected $\delta(a+b)$ with $\nu = 0.3$, $\delta(b-a) = 0$, and $\theta = 0.3\pi$

emerge in the case of $\theta = 0.5\pi$. As a result, a mixed-mode crack should be induced in such a heterogeneous half-plane, which is consistent with the finding in Ref. [31].

Figure 7 gives the moment M that is needed to ensure the cylindrical punch sliding vertically on the surface of the graded half-plane for cases with $\theta = 0.3\pi$ and different friction coefficients μ_f. The intercept on the vertical axis corresponds to the moment that is needed even if the surface friction vanishes. The graded half-plane is reduced to a homogeneous one if $\delta(a+b) = 0$. Then, the moment should be zero if the surface friction coefficient is zero. However, if $\delta(a+b) \neq 0$ and $\theta \neq 0$, the heterogeneity of the graded half-plane still induce a moment in order to keep the cylindrical punch sliding vertically on its surface ever if the surface friction vanishes. As shown in Fig. 7, $\delta(a+b) < 0$ and $\delta(a+b) > 0$ induce moments of opposite directions. Monotonous variations with positive slopes in all the cases infer that the moment of the same direction has been induced with an increasing friction coefficient.

Effects of gradient parameter $\delta(a+b)$ and the gradient variation angle θ on the moment M are given in Figs. 8 and 9, respectively. It is found that the direction of the moment will change if the varying trend of stiffness of the graded half-plane from surface to within changes. However, in both cases, the moment will increase with an increasing gradient variation angle θ no matter whether $\delta(a+b)$ is larger or smaller than zero as shown in Figs. 8 and 9. It will keep a constant for the case with $\delta(a+b) = 0$ and a determined friction coefficient.

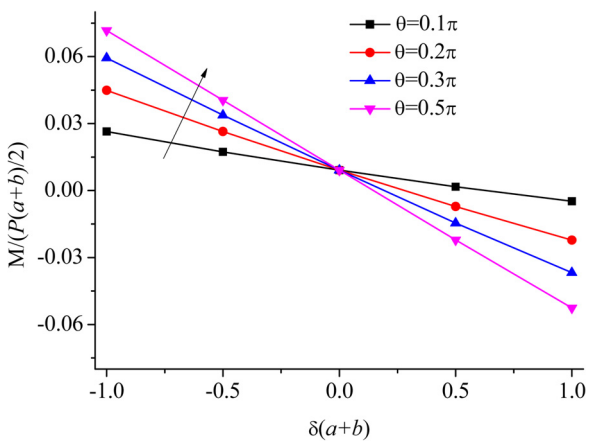

Fig. 8 The moment $M/[P(a+b)/2]$ as a function of the parameter $\delta(a+b)$ for $\mu_f = 0.3$ and different gradient variation angles θ

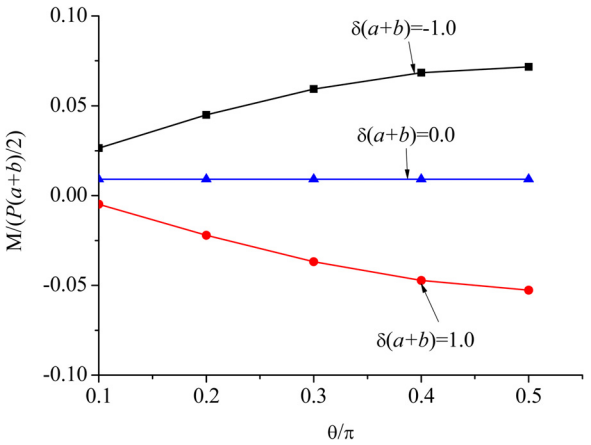

Fig. 9 The moment $M/[P(a+b)/2]$ as a function of the gradient variation angle parameter θ for $\mu_f = 0.3$ and different $\delta(a+b)$

6 Summary

A plane contact model of a cylindrical punch sliding on a graded half-plane with shear modulus gradient varying exponentially in an arbitrary direction is investigated in this paper. With the Fourier integral transform method, distributions of the normal traction and the in-plane surface stress are obtained. Considering effects of the friction coefficient, the gradient variation angle as well as stiffness variation trend of the graded half-plane, we find that (i) the present model is a general one, which can be reduced to the contact problem of a homogeneous half-plane or a laterally graded one; (ii) surface of the graded half-plane with a relatively small friction coefficient or a decreasing stiffness from surface to within is helpful for preventing crack initiation during sliding contact; (iii) the smaller the gradient variation angle, the smaller the in-plane tensile stress near the trailing edge is; and (iv) proper combination of the friction coefficient, gradient parameter, and the gradient variation angle could reduce or avoid effectively the additional moment for stable sliding. The result should be helpful for the design of novel graded materials with strong surface abrasion resistance.

Acknowledgment

P. Chen and J. Peng thank the support of NSFC (Grant Nos. 11402292 and 11404393), Natural Science Foundation of Jiangsu Province (Grant No. BK20140179), the Fundamental Research Funds for the Central Universities (Grant No. 2014QNA73.); S. Chen thanks the support of NSFC (Grant Nos. 11125211 and 11372317) and the 973 Nano-project (2012CB937500).

Appendix A

Coefficients in Eq. (7) are as follows:

$$n_1(\alpha) = -\frac{\Delta_1}{2} - \frac{\sqrt{\Delta_1^2 + 4(\alpha^2 + i\alpha\Delta_2)}}{2},$$
$$n_2(\alpha) = -\frac{\Delta_3}{2} - \frac{\sqrt{\Delta_3^2 + 4(\alpha^2 + i\alpha\Delta_4)}}{2} \quad \text{(A1}a\text{)}$$

$$n_3(\alpha) = -\frac{\Delta_1}{2} + \frac{\sqrt{\Delta_1^2 + 4(\alpha^2 + i\alpha\Delta_2)}}{2},$$
$$n_4(\alpha) = -\frac{\Delta_3}{2} + \frac{\sqrt{\Delta_3^2 + 4(\alpha^2 + i\alpha\Delta_4)}}{2} \quad \text{(A1}b\text{)}$$

$$\Delta_1 = \beta\sqrt{\frac{3-\kappa}{\kappa+1}} + \gamma, \quad \Delta_2 = \beta - \gamma\sqrt{\frac{3-\kappa}{\kappa+1}},$$
$$\Delta_3 = \gamma - \beta\sqrt{\frac{3-\kappa}{\kappa+1}}, \quad \Delta_4 = \beta + \gamma\sqrt{\frac{3-\kappa}{\kappa+1}} \tag{A1c}$$

and $m_j(\alpha)$ for each $n_j(\alpha)$ ($j = 1, \ldots, 4$) can be given as

$$m_j(\alpha) = \frac{[2i\alpha - \beta(3-\kappa)]n_j + i(\kappa-1)\alpha\gamma}{(\kappa-1)n_j^2 + (\kappa-1)\gamma n_j - (\kappa+1)\alpha(\alpha+i\beta)} \tag{A2}$$

Appendix B

The kenerls $K_{ij}(x,r)$ in Eqs. (14) and (15) are expressed as

$$K_{11}(x,r) = \int_0^{+\infty}\left[\alpha N_{11}(\alpha) + \frac{\kappa+1}{4}\right]\sin[\alpha(r-x)]d\alpha \tag{B1a}$$

$$K_{12}(x,r) = -i\int_0^{+\infty}\left[\alpha N_{12}(\alpha) - i\frac{\kappa-1}{4}\right]\cos[\alpha(r-x)]d\alpha \tag{B1b}$$

$$K_{21}(x,r) = -i\int_0^{+\infty}\left[\alpha N_{21}(\alpha) + i\frac{\kappa-1}{4}\right]\cos[\alpha(r-x)]d\alpha \tag{B1c}$$

$$K_{22}(x,r) = \int_0^{+\infty}\left[\alpha N_{22}(\alpha) + \frac{\kappa+1}{4}\right]\sin[\alpha(r-x)]d\alpha \tag{B1d}$$

where $N_{jk}(\alpha)$ $(j,k = 1,2)$ are the corresponding four elements in matrix $\mathbf{N}(\alpha)$, i.e.,

$$\mathbf{N}(\alpha) = \begin{bmatrix} m_1 & m_2 \\ 1 & 1 \end{bmatrix} \bullet \begin{bmatrix} \mu/(m_1 n_1 - i\alpha) & \mu/(m_2 n_2 - i\alpha) \\ \mu/\{(\kappa-1)[-i\alpha m_1(3-\kappa) + n_1(1+\kappa)]\} & \mu/\{(\kappa-1)[-i\alpha m_2(3-\kappa) + n_2(1+\kappa)]\} \end{bmatrix}^{-1} \tag{B2}$$

Appendix C

As a special case, solutions of the contact problem of a rigid cylindrical punch sliding on a homogeneous half-plane are

$$\sigma_{yy}(x,0) = -\frac{4\mu_0}{\kappa+1}\frac{\sin\pi\beta_1}{R}(a-x)^{\beta_1}(x+b)^{\beta_2} \tag{C1}$$

$$\sigma_{xx}(x,0) = -\frac{4\mu_0}{\kappa+1}\frac{\sin\pi\beta_1}{R} \times \begin{cases} (a-x)^{\beta_1}(x+b)^{\beta_2} + \dfrac{\mu_f}{\pi}L_0, & -b \le x \le a, \\ \dfrac{\mu_f}{\pi}L_0, & x < -b, x > a \end{cases} \tag{C2}$$

where

$$L_0(x) = \frac{\pi}{\sin\pi\beta_1}\begin{cases} -2(a-x)^{\beta_1}(-x-b)^{\beta_2} - 2x + a - b + (\beta_1 - \beta_2)(a+b), & x < -b, \\ 2(a-x)^{\beta_1}(x+b)^{\beta_2}\cos\pi\beta_1 - 2x + a - b + (\beta_1 - \beta_2)(a+b), & -b \le x \le a, \\ 2(x-a)^{\beta_1}(x+b)^{\beta_2} - 2x + a - b + (\beta_1 - \beta_2)(a+b), & x > a \end{cases} \tag{C3}$$

and

$$a = \frac{\beta_2}{\beta_1}b \tag{C4}$$

References

[1] Suresh, S., and Mortensen, A., 1998, *Fundamentals of Functionally Graded Materials*, IOM Communications, London.
[2] Suresh, S., 2001, "Graded Materials for Resistance to Contact Deformation and Damage," Science, **292**(5526), pp. 2447–2451.
[3] Suresh, S., Giannakopoulos, A. E., and Alcala, J., 1997, "Spherical Indentation of Compositionally Graded Materials: Theory and Experiments," Acta Mater., **45**(4), pp. 1307–1321.
[4] Jitcharoen, J., Padture, N. P., Giannakopoulos, A. E., and Suresh, S., 1998, "Hertzian-Crack Suppression in Ceramics With Elastic-Modulus-Graded Surfaces," J. Am. Ceram. Soc., **81**(9), pp. 2301–2308.
[5] Krumova, M., Klingshirn, C., Haupert, F., and Friedrich, K., 2001, "Microhardness Studies on Functionally Graded Polymer Composites," Compos. Sci. Technol., **61**(4), pp. 557–563.
[6] Giannakopoulos, A. E., and Suresh, S., 1997, "Indentation of Solids With Gradients in Elastic Properties.1. Point Force," Int. J. Solids Struct., **34**(19), pp. 2357–2392.
[7] Giannakopoulos, A. E., and Suresh, S., 1997, "Indentation of Solids With Gradients in Elastic Properties. 2. Axisymmetric Indentors," Int. J. Solids Struct., **34**(19), pp. 2393–2428.
[8] Guler, M. A., and Erdogan, F., 2004, "Contact Mechanics of Graded Coatings," Int. J. Solids Struct., **41**(14), pp. 3865–3889.
[9] Guler, M. A., and Erdogan, F., 2006, "Contact Mechanics of Two Deformable Elastic Solids With Graded Coatings," Mech. Mater., **38**(7), pp. 633–647.
[10] Guler, M. A., and Erdogan, F., 2007, "The Frictional Sliding Contact Problems of Rigid Parabolic and Cylindrical Stamps on Graded Coatings," Int. J. Mech. Sci., **49**(2), pp. 161–182.
[11] El-Borgi, S., Abdelmoula, R., and Keer, L., 2006, "A Receding Contact Plane Problem Between a Functionally Graded Layer and a Homogeneous Substrate," Int. J. Solids Struct., **43**(3–4), pp. 658–674.
[12] Rhimi, M., El-Borgi, S., Said, W. B., and Jemaa, F. B., 2009, "A Receding Contact Axisymmetric Problem Between a Functionally Graded Layer and a Homogeneous Substrate," Int. J. Solids Struct., **46**(20), pp. 3633–3642.
[13] Choi, H. J., and Paulino, G. H., 2008, "Thermoelastic Contact Mechanics for a Flat Punch Sliding Over a Graded Coating/Substrate System With Frictional Heat Generation," J. Mech. Phys. Solids, **56**(4), pp. 1673–1692.

[14] Choi, H. J., and Paulino, G. H., 2010, "Interfacial Cracking in a Graded Coating/Substrate System Loaded by a Frictional Sliding Flat Punch," Proc. R. Soc. A, **466**(2115), pp. 853–880.
[15] Ke, L. L., and Wang, Y. S., 2006, "Two-Dimensional Contact Mechanics of Functionally Graded Materials With Arbitrary Spatial Variations of Material Properties," Int. J. Solids Struct., **43**(18–19), pp. 5779–5798.
[16] Ke, L. L., and Wang, Y. S., 2007, "Two-Dimensional Sliding Frictional Contact of Functionally Graded Materials," Eur. J. Mech. A. Solids, **26**(1), pp. 171–188.
[17] Chen, P., and Chen, S., 2012, "Contact Behaviors of a Rigid Punch and a Homogeneous Half-Space Coated With a Graded Layer," Acta Mech., **223**(3), pp. 563–577.
[18] Chen, P., and Chen, S., 2013, "Partial Slip Contact Between a Rigid Punch With an Arbitrary Tip-Shape and an Elastic Graded Solid With a Finite Thickness," Mech. Mater., **59**(1), pp. 24–35.
[19] Chen, P., Chen, S., and Peng, Z., 2012, "Thermo-Contact Mechanics of a Rigid Cylindrical Punch Sliding on a Finite Graded Layer," Acta Mech., **223**(12), pp. 2647–2665.
[20] Giannakopoulos, A. E., and Pallot, P., 2000, "Two-Dimensional Contact Analysis of Elastic Graded Materials," J. Mech. Phys. Solids, **48**(8), pp. 1597–1631.
[21] Chen, S. H., Yan, C., and Soh, A., 2009, "Adhesive Behavior of Two-Dimensional Power-Law Graded Materials," Int. J. Solids Struct., **46**(18–19), pp. 3398–3404.
[22] Chen, S. H., Yan, C., Zhang, P., and Gao, H. J., 2009, "Mechanics of Adhesive Contact on a Power-Law Graded Elastic Half-Space," J. Mech. Phys. Solids, **57**(9), pp. 1437–1448.
[23] Guo, X., Jin, F., and Gao, H. J., 2011, "Mechanics of Non-Slipping Adhesive Contact on a Power-Law Graded Elastic Half-Space," Int. J. Solids Struct., **48**(18), pp. 2565–2575.
[24] Jin, F., Guo, X., and Gao, H., 2013, "Adhesive Contact on Power-Law Graded Elastic Solids: The JKR-DMT Transition Using a Double-Hertz Model," J. Mech. Phys. Solids, **61**(12), pp. 2473–2492.
[25] Jin, F., Guo, X., and Zhang, W., 2013, "A Unified Treatment of Axisymmetric Adhesive Contact on a Power-Law Graded Elastic Half-Space," ASME J. Appl. Mech., **80**(6), p. 061024.
[26] Dag, S., Guler, M. A., Yildirim, B., and Ozatag, A. C., 2009, "Sliding Frictional Contact Between a Rigid Punch and a Laterally Graded Elastic Medium," Int. J. Solids Struct., **46**(22–23), pp. 4038–4053.
[27] Dag, S., Guler, M. A., Yildirim, B., and Ozatag, A. C., 2013, "Frictional Hertzian Contact Between a Laterally Graded Elastic Medium and a Rigid Circular Stamp," Acta Mech., **224**(8), pp. 1773–1789.
[28] Galin, L. A., 2008, *Contact Problems: The Legacy of L. A. Galin*, Springer, New York.
[29] Chen, P., and Chen, S., 2013, "Thermo-Mechanical Contact Behavior of a Finite Graded Layer Under a Sliding Punch With Heat Generation," Int. J. Solids Struct., **50**(7–8), pp. 1108–1119.
[30] Dag, S., and Erdogan, F., 2002, "A Surface Crack in a Graded Medium Loaded by a Sliding Rigid Stamp," Eng. Fract. Mech., **69**(14–16), pp. 1729–1751.
[31] Konda, N., and Erdogan, F., 1994, "The Mixed Mode Crack Problem in a Nonhomogeneous Elastic Medium," Eng. Fract. Mech., **47**(4), pp. 533–545.